Sensors & Transducers, Vol. 193, Issue 10, October 2015, pp. 80-85

Sensors & Transducers

http://www.sensorsportal.com

Analysis of the Planar Electrode Morphology Applied to Zeolite Based Chemical Sensors

[1] Luiz Eduardo BENTO RIBEIRO, [2] Glaucio Pedro de ALCÂNTARA, [2] Cid Marcos GONÇALVES ANDRADE, [1] Fabiano FRUETT

[1] School of Electrical and Computer Engineering of State University of Campinas, Campinas, Brazil

[2] Department of Chemical Engineering of State University of Maringá, Paraná, Brazil

E-mail: luizebr@dsif.fee.unicamp.br, fabiano@dsif.fee.unicamp.br

Received: 31 August 2015 /Accepted: 5 October 2015 /Published: 30 October 2015

Abstract: In order to improve the zeolite chemical sensors sensibility, three different electrode structures are compared in this work: conventional interdigitated electrodes (IDE), serpentine electrodes (SRE) and ring-shaped electrodes (RSE). Simulation results and experimental characterization of these electrodes showed that ring-shaped electrodes have a slight capacitance increase per unit of area. When used as a zeolite chemical sensor, the ring-shaped electrodes prove to be more suitable since they take advantage of a better usage of the drop distribution and a better capacitance per area ratio. *Copyright © 2015 IFSA Publishing, S. L.*

Keywords: Interdigitated electrodes, Ring-shaped electrodes, Serpentine electrodes, Chemical sensors, Electrode structure, Interdigital electrodes, Zeolite.

1. Introduction

IDE as capacitive microstructures have been widely used in electronics applications such as surface acoustic wave devices [1-2], thin-film acoustic electronic transducers [3], tunable devices [4], dielectric spectroscopy [5], dielectric studies on thin films [6], humidity and chemical sensors [7-9], etc. They possess interesting features, such as signal strength control by changing its dimensions, multiple physical effects in the same structure, simplified modeling in two dimensions when the aspect ratio of the electrode length to the space wavelength IDE is large, and can be used in a wide range of frequencies [10]. Moreover, it can be manufactured using inert substrates with multiple materials with different fabrication processes, or even microfluidic compatible. Capacitive microstructures used as chemical sensor, typically have one sensitive layer deposited over the electrodes. Polymers have been used for organic vapor sensing because they exhibit rapid reversible vapor sorption and are easy to apply as thin or thick films by a variety of techniques [10]. The polymer layer can be chosen according to its affinity to a particular molecule or set of molecules one wishes to detect. If several sensors with different polymer layers are used to make a sensor array it is then possible to evaluate complex organic vapor samples. These sensor arrays can be part of a so-called electronic nose. Another possibility is the use of flexible substrates such as sensing element. As an example the use of polyimide [11] and plastic foil [12].

Interdigitated electrodes analytical characterization have been received many efforts in order to improve their capacitance by exploring their geometrical parameters [13]. Igreja et al developed a theoretical model of capacitance for this structure [14]. These capacitors have also been simulated using different tools. They have typically been adopted as a

sensor because of the low-power consumption of capacitive transduction mechanism and being compact with a large contact area and relative ease of manufacture. Some authors have analyzed other morphologies such as serpentine, spiral and concentric rings electrodes, in order to improve design performance. Moreover, aside from the different morphologies, several strategies have been employed to increase and improve its ability as a sensor, for example the deposition of a more sensitive layer on the electrodes. The sensor can also have its selectivity improved by the deposition of compounds such as zeolite for detection of air humidity or gases [15].

In this work, we study different geometries of electrodes instead of the materials used to maximize capacitance per area. We can thus improve the sensitivity of capacitive sensors by increasing the total capacitance of capacitive microstructures. Here, we compare the conventional IDE, the serpentine electrodes (SRE) and ring-shaped electrodes (RSE). These electrodes are compared in detail as generic capacitive transducers by numerical simulations. In these simulations, the geometric parameters that most influence on the total capacitance are shown. We measure the capacitance of these thin-film electrodes made of titanium and gold on a glass substrate. After that, we compare the experimental results with the theoretical analysis, including simulations. Finally, we compared the influence of such geometries under a LTA structured zeolite layer.

In Section 2, the different electrodes designs and their geometrical parameters are shown. They are the main data to the numerical simulation, which is explained in the Section 3. The fabrication process is described in Section 4, while the zeolite properties and deposition method are described in Section 5. Subsequently, the values of electrical and geometrical characterization are shown in Section 6. The results are compared and discussed in Section 7. Finally, the conclusion is presented in Section 8.

2. Methods and Materials

The layouts of some interdigitated electrode pairs are shown in Fig. 1. Although they were designed with the same area, each structure has a particular capacitance. Therefore, they have different sensitivities as capacitive transducer only because of their different geometric structure.

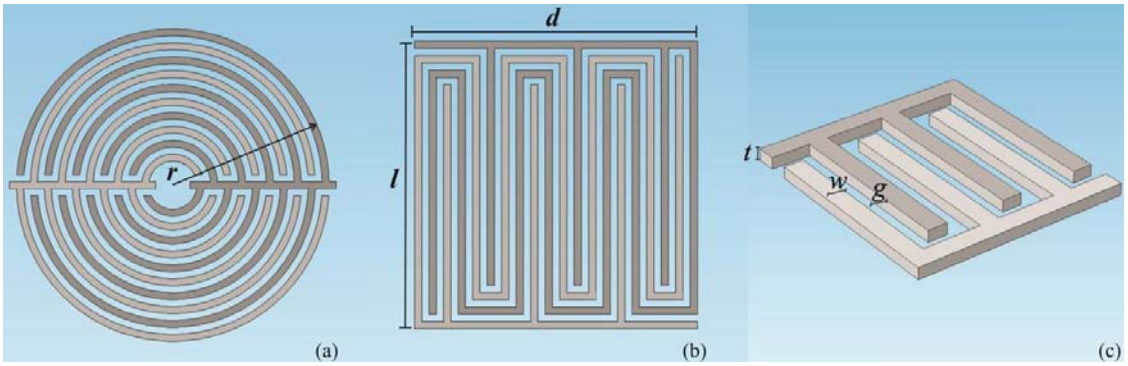

Fig. 1. Ring-shape electrode (a); serpentine electrode (b); and interdigitated electrode (c) structures and used parameters.

We simulate the capacitive structures of IDE, SRE and RSE with the same area, same substrate and the same top layer, calculating and comparing the capacitance of each structure using the multiphysics numerical simulator: COMSOL Multiphysics (Comsol, Inc., Stockholm, Sweden). This software, based on partial differential equations with the finite element method has been used in the literature to calculate distribution of potential field in similar structures. Fig. 2 depicts the simulated structure showing the 3D multislice view of the electrical potential distribution around RSE with 20 fingers.

Multiple simulations were performed to compare dimensions that are relevant to increase the difference between the capacitances. The main geometrical parameters analyzed are the electrode length, the gap between the electrodes, the electrode width (always kept as same value as gap), the thickness of electrodes and the number of fingers.

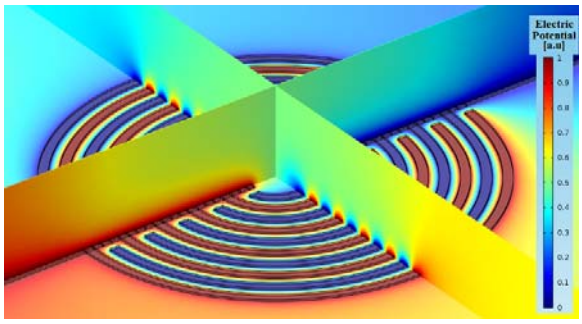

Fig. 2. Distribution of potential field in a 3D RSE structure.

The electrical properties of the substrate and the top layer are also included in the simulator. Because of the differences between the vertical and horizontal dimensions (millimeters to micrometers) critical to reduce the time simulation, we have applied the extrapolation method, presented in the Rivadeneyra work [16]. The thickness has been set to 20 % of electrode width.

3. Numerical Simulation

We have performed different numerical simulations comparing the calculated DC capacitance of IDE, SRE and RSE structures always with the same distance between digits, surface area and same materials and manufacturing process. There are multiple geometrical factors that can be varied in the simulations, but for the sake of clarity, we focus on some of them, keeping fixed the rest. Since the goal is maintaining reduced the surface area of electrodes, we define different widths and distances between digits of the structures given that the lowest safe distance to our manufacturing process is 10 µm. Therefore, we have used the number, length and width of fingers and the thickness of the deposited metal film as simulation parameters. Table 1 is a summary of these geometric parameters used for simulation. Remember that fabricated structures for each type of electrode, SRE, IDE and RSE, was made with three distances between digits (10 µm, 20 µm and 50 µm) but the number of electrodes and the thickness of the metal thin film was kept constant.

Table 1. Geometrical Parameters of Planar Electrodes Pairs.

Para-meters	Electrode type			Descripti-on
	RSE	***SRE***	***IDE***	
w	10-50 µm	10-50 µm	10-50 µm	Finger width
g	10-50 µm	10-50 µm	10-50 µm	Gap between fingers
t	2-10 µm	2-10 µm	2-10 µm	Metal film thickness
l	600-800 µm	600-800 µm	-	Structure length
d	600-800 µm	600-800 µm	-	Structure width
r	-	-	0.6-3.02 mm	Electrode external radium
n	20-50	20-50	20-50	Number of electrodes

The first important result was that the capacitance to RSE was the highest in all comparisons. For example, simulating the capacitor with w = 10 µm, t = 2 µm and 20 electrodes we obtain 2.47 pF for RSE while the capacitance for the SRE was 2.45 pF and the capacitance for IDE was 2.44 pF. This means an increase of capacitance of 30 fF between the RSE and the IDE. Whereas electrodes are used as capacitive transducers, the fact of the geometrical factor RSE be higher than in other structures means that the sensitivity of the sensor will always be larger using the same area. Furthermore, the capacitance and the increase in sensitivity will increase proportionally. After that, we calculate the numerical capacitances in order to improve the performance of RSE.

Influence of the width of the electrodes (10 to 50 µm) with aspect ratio of the electrode/thickness of the thin film of 5/1 was evaluated for the RSE, SRE and IDE with 20 digits. The results showed a slope of 161.1 fF for each micrometer added to the width of the electrodes to the RSE, a slope of 160.7 fF/µm for the SRE and 159.3 fF/µm for the IDE. Remembering that the surface area of each structure was kept the same for each electrode width.

Electrode length contribution (400 to 800 µm) was been evaluated for IDE and SRE electrode with 20 fingers and 10 µm of finger width. Results showed the slope of 4.99 fF/µm for the SRE and 4.74 fF for the IDE.

We also have performed the contribution of finger numbers (n) in each structure. The results are presented in Fig. 3, as this contribution is nonlinear.

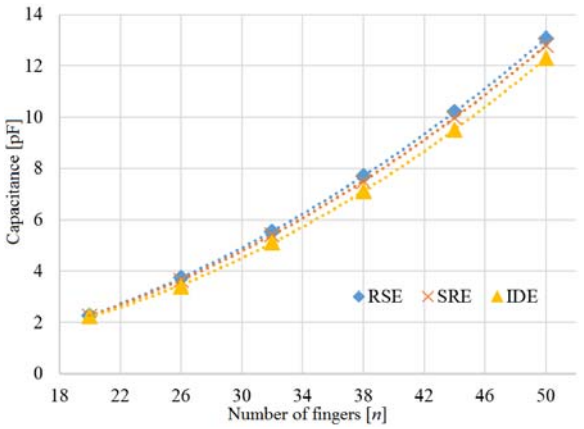

Fig. 3. Capacitance vs. number of fingers of RSE, SRE and IDE.

4. Fabrication Process

The electrodes fabrication started with the production of the electrode masks where the IDE, SRE and RSE were designed using high-resolution direct writing photolithography with a laser beam. In the next step, a photoresist layer was deposited onto a square optical glass plate (60 mm side Kodak 1A High Resolution Glass) and patterned by conventional ultraviolet light (UV) photolithographic method following the electrodes masks. The UV exposures were carried out in a MJB-3 UV300 contact mask aligner (Karl-Suss, Garching, Germany). Titanium-gold (TiAu) thin films, deposited with a Leybold Univex 300 ebeam

evaporator (Cologne, Germany), were used as electrode materials. After thin-film depositions, by the lift-off technic, the devices were immersed in acetone to remove the photoresist layer and excess of metal, leaving the patterned electrodes on the glass surface [7].

5. Characterization

For the experimental characterization the nominal capacitance target was 2 pF, taking into account the minimum distance between electrodes of 10 µm. Structures with electrode width of 50µm have a total area of 28.26 mm², and their dimensions are g = 50 µm, l = 5.95 mm, d = 4.75 mm and r = 3.02 mm. The area is 4.52 mm² for structures with w = 20 µm, g = 20 µm, l = 2.38 mm, d = 1.90 mm and r = 1.21 mm. Structures with w = 10 µm, minimum secure dimension to our fabrication process, the area is 1.13 mm² (g = 10 µm, l = 1.19 mm, d = 0. 95 mm and r = 0.60 mm).

The geometric inspection of the fabricated structures was performed using the Olympus BX60 microscope as shown in Fig. 4.

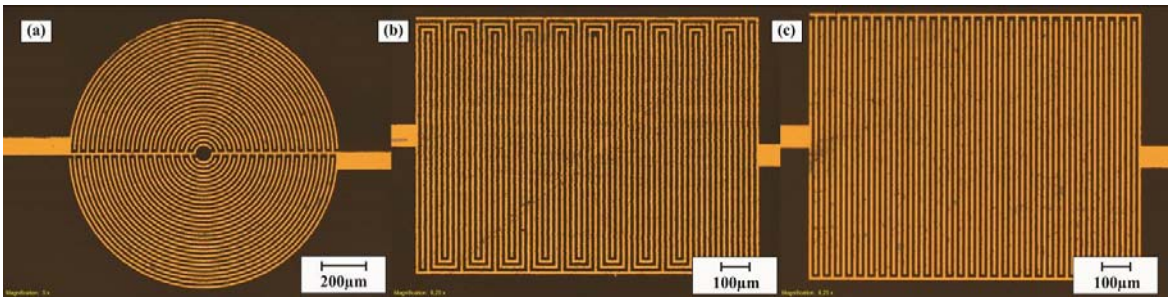

Fig. 4. Fabricated RSE (a); SRE (b); and IDE (c) structures.

Electrical characterization has been carried out by measuring their capacitance and parallel resistance using the four-wire measurement with a HP 4284A impedance analyzer (Agilent Tech., Santa Clara, CA, USA). The applied excitation voltage was VAC = 1 V and VDC = 0 V. The frequency sweep of analysis was from 100 Hz to 1 MHz. The four-point method was used to minimize the contribution of stray capacitances.

6. Zeolite Deposition

The zeolite layers were prepared using micro-drop deposition. A top view of zeolite over electrodes can be observed in the Fig. 5. The process first step involves suspension of the crystals in alcohol. We placed 0.1 g of the zeolite crystals with 10 ml of isopropyl alcohol into a vessel. After that, the vessel was placed into a sonic bath for 10 minutes. The bath make the suspension homogenous, allowing agglomerations to sink to the bottom of the vessel leaving single crystals dispersed.

Using a micro-syringe, a single droplet (10 µl) of the solution was carefully deposited on to the electrodes under a low magnification microscope. After 10 minutes, the isopropyl alcohol evaporated and the crystals adhered to the surface by electrostatic forces. The evaporation of this droplet takes place leaving a zeolite deposit on the electrodes. The process was repeated until around 100 µl was achieved (usually repeated 10 times) [15].

The used LTA structured zeolite (zeolite A) is built up of two types of arrangements; 8 tetrahedra in a cubic shape and 24 tetrahedra in an octahedron shape. The framework is formed by the connection of every cube corner to the octahedrons creating caged cavities in-between. Zeolite A is a low-silica based zeolite and therefore has a high cation concentration to compensate for the reduction in charge [17]. The Si/Al ratio is around 1 making this type of zeolite a fairly hydrophilic material. The pore size is around 4 angstroms, the cage diameter is 11.5 angstroms and the pore volume is around 0.30 cc/g [18].

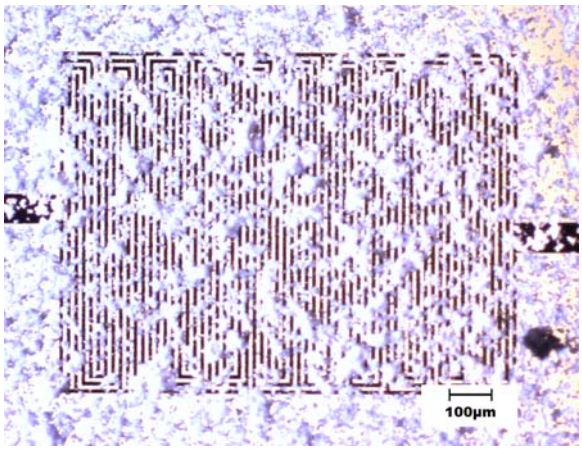

Fig. 5. Microstructure during the zeolite deposition process.

7. Experimental Results

Measured and the simulated values of the capacitances are in agreement, as shown in Table 2.

The measurements were carried out in room conditions (50 % RH and 25ºC) at 100 kHz.

Table 2. Numerical vs. Experimental Capacitance.

Finger width (μm)	Numerical simulation (pF)		
	RSE	***SRE***	***IDE***
10	2.4667	2.4446	2.4362
20	4.0906	4.0653	4.0345
50	8.9122	8.8723	8.8091
	Experimental measurement (pF)		
	RSE	***SRE***	***IDE***
10	2.2332	2.2141	2.1917
20	4.2949	4.2667	4.2412
50	10.5385	9.9979	9.7105

Capacitance measured values have a maximum of 12 % discrepancy compared to the simulated results. This difference is due to the capacitance of contacts pads that were not included in the simulation and the variability of the fabrication process.

After the zeolite deposition, we also measured the percentage of the capacitance increment when the structures are with and without the zeolite layer. For the ring-shape electrode the capacitance with zeolite layer incremented 139 % (2.39 times) of that without zeolite. In case of the interdigitated electrodes, the capacitance with zeolite layer incremented 44 % (1.44 times) in comparison of that without zeolite.

This preliminary study indicates that the sensibility of a zeolite chemical sensor can be also improved by changing the capacitive microstructure. However, when in contact with the liquid or gas under analysis, the total impedance must be modeled to comprise effects such as double layer capacitance and interfacial polarization phenomenon.

8. Conclusion

A comparison between the capacitances under different geometric parameters of RSE, SRE and the conventional IDE was shown on this work. Numerical simulations of the capacitance have been carried out to calculate the differences between them due exclusively to their geometrical characteristics at constant area. In these conditions, we have shown a slight capacitance increase for the ring-shaped electrodes against the serpentine electrodes and the conventional interdigitated electrodes.

We have validated the numerical results by experimental characterization of ring-shaped, serpentine and interdigitated structures capacitance. Experimental results verified the capacitive differences between the three structures with same area, for 10 μm, 20 μm and 50 μm of finger width. Moreover, ring-shape electrode presents a geometrical morphology that allows the better usage of its area. It is a promising base electrode mainly when used as sensor in application that involves dripping of substances under analysis or dripping of selective/sensitive substances like zeolite.

While the capacitance of the interdigitated electrodes with zeolite layer is 1.44 times greater, the ring-shape electrodes is 2.39 times greater. This preliminary study with zeolite deposition over the electrodes show us that the total capacitance can be further enhanced by the electrode geometry.

Acknowledgements

The authors acknowledge the Center for Semiconductor Components (CCS), the Multi-User Laboratory of IFGW (LAMULT), the Device Research Laboratory (LPD) and the Brazilian Synchrotron Light Laboratory (LNLS). Financial support for this project was provided by the National Council for Scientific and Technological Development (CNPq) and the São Paulo State Research Support Foundation (FAPESP) inside the National Institute for Science and Technology of Micro and Nanoelectronic Systems (INCT NAMITEC) project.

References

[1]. M. I. Rocha-Gaso, C. March-Iborra, Á. Montoya-Baides, A. Arnau-Vives, Surface generated acoustic wave biosensors for the detection of pathogens: A review, *Sensors*, Vol. 9, No. 7, 2009, pp. 5740-5769.

[2]. N. A. Ramli, A. N. Nordin, Design and modeling of MEMS SAW resonator on Lithium Niobate, in *Proceedings of the 4th International Conference on Mechatronics (ICOM'11)*, 2011, pp. 1-4.

[3]. M. W. Kim, Y. H. Song, J. B. Yoon, Modeling, fabrication and demonstration of a rib-type cantilever switch with an extended gate electrode, *Journal of Micromechanics and Microengineering*, Vol. 21, 2011, 115009.

[4]. R. Mahameed, A. M. El-Tanani, G. M. Rebeiz, A zipper RF MEMS tunable capacitor with interdigitated RF and actuation electrodes, *Journal of Micromechanics and Microengineering*, Vol. 20, No. 3, 2010, 035014.

[5]. Heileman, Khalil, Jamal Daoud, Maryam Tabrizian, Dielectric spectroscopy as a viable biosensing tool for cell and tissue characterization and analysis, *Biosensors and Bioelectronics*, Vol. 49, 2013, pp. 348-359.

[6]. Z. Chen, A. Sepúlveda, M. D. Ediger, R. Richert, Dielectric spectroscopy of thin films by dual-channel impedance measurements on differential interdigitated electrode arrays, *The European Physical Journal B - Condensed Matter and Complex Systems*, Vol. 85, No. 8, 2012, pp. 1-5.

[7]. L. E. B. Ribeiro, M. H. Piazzetta, A. L. Gobbi, J. S. Costa, J. A. F. da Silva, and F. Fruett, Fabrication and Characterization of an Impedance Micro-Bridge for Lab-on-a-Chip, *ECS Transactions*, Vol. 31, No. 1, 2010, pp. 155-163.

[8]. Y. Kim, B. Jung, H. Lee, H. Kim, K. Lee, H. Park, Capacitive humidity sensor design based on anodic aluminum oxide, *Sensors and Actuators B: Chemical*, Vol. 141, No. 2, 2009, pp. 441-446.

[9]. A. Rivadeneyra, J. Fernández-Salmerón, J. Banqueri, J. A. López-Villanueva, L. F. Capitan-Vallvey, A. J. Palma, A novel electrode structure compared with interdigitated electrodes as capacitive sensor, *Sensors and Actuators B: Chemical*, Vol. 204, 2014, pp. 552-560.

[10]. J. W. Grate, G. C. Frye, Acoustic wave sensors, *Sensors*, Vol. 2, Issue 1, 1996, pp. 37-83.

[11]. J. Virtanen, L. Ukkonen, T. Bjorninen, L. Sydanheimo, Printed humidity sensor for UHF RFID systems, in *Proceedings of the IEEE Sensors Applications Symposium (SAS'10)*, 2010, pp. 269-272.

[12]. D. Briand, A. Oprea, J. Courbat, N. Bârsan, Making environmental sensors on plastic foil, *Materials Today*, Vol. 14, No. 9, 2011, pp. 416-423.

[13]. L. E. B. Ribeiro, F. Fruett, Analysis of the Planar Electrode Morphology for Capacitive Chemical Sensors, in *Proceedings of the 6th International Conference on Sensor Device Technologies and Applications Analysis (SENSORDEVICES'15)*, Venice, Italy, 23-28 August 2015, pp. 179-182.

[14]. R. Igreja, C. J. Dias, Analytical evaluation of the interdigital electrodes capacitance for a multi-layered structure, *Sensors and Actuators A: Physical*, Vol. 112, No. 2-3, 2004, pp. 291-301.

[15]. M. Urbriztondo, I. Pellejero, A. Rodriguez, M. P. Pina, J. Santamaria, Zeolite-coated interdigital capacitors for humidity sensing, *Sensors and Actuators B: Chemical*, Vol. 157, Issue 1, 2011, pp. 450-459.

[16]. A. Rivadeneyra, J. Fernández-Salmerón, M. Agudo, J. A. López-Villanueva, L. F. Capitan-Vallvey, A. J. Palma, Design and characterization of a low thermal drift capacitive humidity sensor by inkjet-printing, *Sensors and Actuators B: Chemical*, Vol. 195, 2014, pp. 123-131.

[17]. Scott M. Auerbach, Kathleen A. Carrado, Prabir K. Dutta, Handbook of Zeolite Science and Technology, *Marcel Dekker Inc*., New York, Basel, 2003.

[18]. D. W. Breack, Zeolite molecular sieves-structure, chemistry and use, *Robert E. Krieger Publishing Company*, Malabar, Florida, 1984.
